



HAL
open science

Chemical Delivery System of MIBG to the Central Nervous System: Synthesis, ¹¹C-Radiosynthesis, and in Vivo Evaluation

Fabienne Gourand, Delphine Patin, Axelle Henry, Meziiane Ibazizeñe, Martine Dhilly, Fabien Fillesoye, Olivier Tirel, Mihaela-Liliana Tintas, Cyril Papamicael, Vincent Levacher, et al.

► To cite this version:

Fabienne Gourand, Delphine Patin, Axelle Henry, Meziiane Ibazizeñe, Martine Dhilly, et al.. Chemical Delivery System of MIBG to the Central Nervous System: Synthesis, ¹¹C-Radiosynthesis, and in Vivo Evaluation. ACS Medicinal Chemistry Letters, 2019, 10 (3), pp.352-357. 10.1021/acsmchemlett.8b00642 . hal-03020265

HAL Id: hal-03020265

<https://hal.science/hal-03020265v1>

Submitted on 23 Nov 2020

HAL is a multi-disciplinary open access archive for the deposit and dissemination of scientific research documents, whether they are published or not. The documents may come from teaching and research institutions in France or abroad, or from public or private research centers.

L'archive ouverte pluridisciplinaire **HAL**, est destinée au dépôt et à la diffusion de documents scientifiques de niveau recherche, publiés ou non, émanant des établissements d'enseignement et de recherche français ou étrangers, des laboratoires publics ou privés.

1 Chemical Delivery System of MIBG to the Central Nervous System: 2 Synthesis, ¹¹C-Radiosynthesis, and *in Vivo* Evaluation

3 Fabienne Gourand,^{*,‡} Delphine Patin,[‡] Axelle Henry,[†] Méziane Ibazizène,[‡] Martine Dhilly,[‡]
4 Fabien Fillesoye,[‡] Olivier Tirel,[‡] Mihaela-Liliana Tintas,[‡] Cyril Papamicaël,[†] Vincent Levacher,^{*,†}
5 and Louisa Barré[‡]

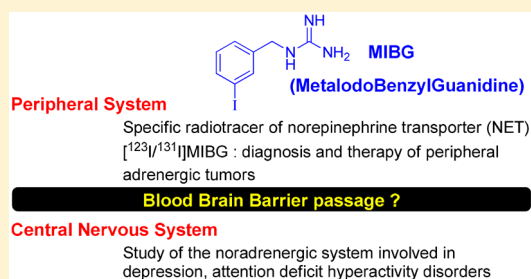
6 [‡]Normandie Univ, UNICAEN, CEA, CNRS, UMR 6030 ISTCT/LDM-TEP group, Bd Henri Becquerel, BP 5229, 14074 Cedex
7 Caen, France

8 [†]Normandie Univ, COBRA, UMR 6014 et FR 3038; Univ Rouen; INSA Rouen; CNRS, IRCOF, 1 rue Tesnière, 76821 Mont Saint
9 Aignan Cedex, France

10 **S** Supporting Information

11 **ABSTRACT:** The norepinephrine transporter (NET) plays an impor-
12 tant role in neurotransmission and is involved in a multitude of
13 psychiatric and neurodegenerative diseases. [¹²³I/¹³¹I]meta-iodobenzyl-
14 guanidine (MIBG) is a widely used radiotracer in the diagnosis and
15 follow-up of peripheral neuroendocrine tumors overexpressing the
16 norepinephrine transporter. MIBG does not cross the blood–brain
17 barrier (BBB), and we have demonstrated the “proof-of-concept” that 1,4-
18 dihydroquinoline/quinolinium salt as chemical delivery system (CDS) is
19 a promising tool to deliver MIBG to the brain. To improve BBB passage,
20 various substituents on the 1,4-dihydroquinoline moiety and a linker
21 between CDS and MIBG were added. A series of CDS-MIBGs **1a–d** was synthesized, labeled with carbon-11, and evaluated *in*
22 *in vivo* into rats. The *in vivo* results demonstrated that, although adding substituents on CDS in **1a–c** is of no benefit for brain
23 delivery of MIBG, the presence of a linker in CDS-MIBG **1d** greatly improved both brain penetration and the release rate of
24 MIBG in the central nervous system.

25 **KEYWORDS:** Central nervous system, norepinephrine transporter, MIBG, radiosynthesis, redox chemical delivery system,
26 1,4-dihydroquinolines carriers



27 **T**he *in vivo* expression of norepinephrine transporter
28 (NET) is mostly established in the central and peripheral
29 sympathetic nervous system. Several different radiotracers for
30 clinical imaging of NET expression were developed.

31 Among them, meta-iodobenzylguanidine (MIBG) is struc-
32 turally similar to the neurotransmitter norepinephrine, and
33 [¹²³I]MIBG single photon emission computed tomography
34 (SPECT) imaging studies are the most accurate method for
35 detection of catecholamine-secreting tumors including neuro-
36 endocrine tumors such as pheochromocytoma and neuro-
37 blastoma.^{1–3}

38 Moreover, MIBG was also radiolabeled with iodine-131 for
39 radiotherapy to treat neuroendocrine tumors. Positron
40 emission tomography (PET) is more accurate and has the
41 potential to be more sensitive and to provide better image
42 resolution. In this context, efforts to develop MIBG analogs
43 labeled with a positron emitter remain of great interest, and
44 several ¹⁸F-labeled benzylguanidine analogs have already been
45 developed for PET imaging of NET expression. Recently, the
46 radiotracer meta-[¹⁸F]Fluorobenzylguanidine ([¹⁸F]MFBG)
47 has shown to be a very promising PET candidate leading to
48 successful clinical investigations.^{4–7} Dysregulation of NET is
49 implicated in various neuropsychiatric disorders such as

depression, anxiety, attention deficit hyperactivity disorders
50 (ADHD), Parkinson’s disease, Alzheimer’s disease, and
51 epilepsy. As the NET plays an important role in the central
52 nervous system (CNS), the use of MIBG or MIBG analogs in
53 brain imaging needs to be explored. However, MIBG is unable
54 to cross the blood–brain-barrier (BBB). Guilloteau et al. have
55 compared the uptake and release of radioiodinated meta-
56 iodobenzylguanidine ([¹²⁵I]MIBG) and tritiated norepineph-
57 rine ([³H]NE) in different regions of the rat brain. The authors
58 found comparable regional distribution of [³H]NE and
59 [¹²⁵I]MIBG uptake in the rat brain.⁸ A chemical delivery
60 system (CDS) designed for MIBG able to cross the BBB would
61 provide a potential imaging marker to visualize the NET in the
62 brain (Figure 1). In the literature, Bodor et al. have developed
63 an interesting CDS based on a lipophilic 1,4-dihydropyridine
64 able to cross the lipophilic BBB.^{9,10} Then, the 1,4-
65 dihydropyridine system is oxidized into the CNS to a
66 hydrophilic pyridinium species, which cannot cross back the
67 BBB (named as “the locked in effect”). A subsequent
68

Received: December 18, 2018

Accepted: February 15, 2019

Published: February 15, 2019

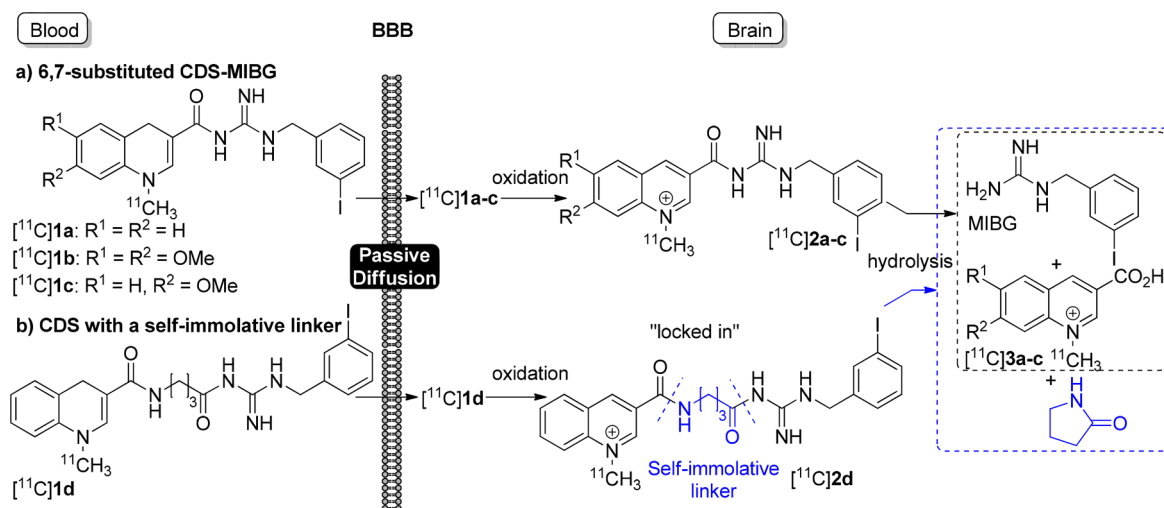
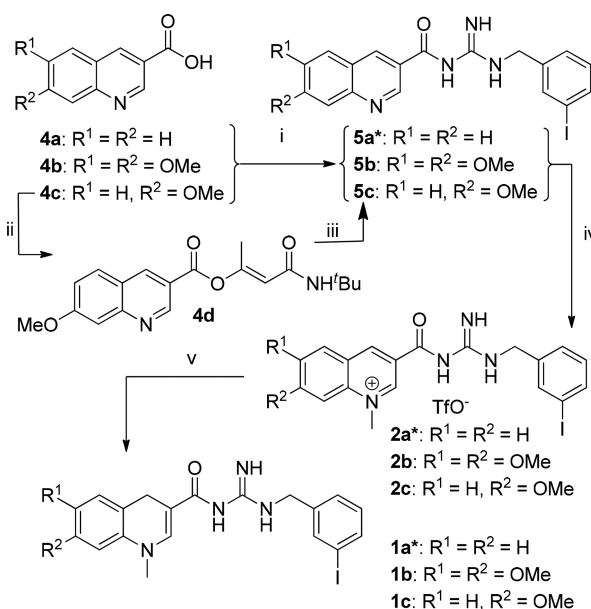


Figure 1. Development of a ^{11}C -chemical delivery system of MIBG into the CNS.

69 hydrolysis releases the active compound, which can then act
 70 directly on the target into the CNS. By using this approach,
 71 Bodor et al. have targeted many drugs to the CNS.^{11–14} Later,
 72 Levacher et al. have solved many drawbacks related to this
 73 CDS by means of 1,4-dihydroquinolines instead of 1,4-
 74 dihydropyridines. However, although mainly drugs were
 75 successfully targeted using this strategy, very few reports deal
 76 with the use of this CDS to target radiotracers into the brain. A
 77 survey of the literature indicated that, aside from our previous
 78 work on MIBG,^{15,16} only a single research article¹⁷ explored
 79 the potential of this appealing CDS approach to deliver a
 80 radiolabeled agent into the CNS. As far as our preliminary
 81 research work on MIBG is concerned, our initial work focused
 82 on the radiolabeling with carbon-11 of the CDS in order to
 83 validate the concept described previously. The results of the *in*
 84 *vivo* studies were highly encouraging, supporting our working
 85 hypothesis that the dihydroquinoline system may possibly be a
 86 promising CDS to target MIBG to brain tissues. Indeed, after
 87 *in vivo* injection into rats of $[^{11}\text{C}]$ CDS-MIBG ($[^{11}\text{C}]1\text{a}$), the
 88 passage of $[^{11}\text{C}]1\text{a}$ through the BBB has been demonstrated as
 89 well as the presence of MIBG in the brain. However, this
 90 chemical delivery system has some limitations: (1) a moderate
 91 brain penetration has been measured, and (2) the oxidation
 92 kinetics of $[^{11}\text{C}]1\text{a}$ was quite slow since more than 50% was
 93 still present in rat brain at 45 min post injection. For these
 94 reasons, this CDS still needed to be optimized before being
 95 applied to radioiodinated MIBG. This Letter will focus on the
 96 preparation and *in vivo* evaluation of new 1,4-dihydroquino-
 97 line-MIBG systems $[^{11}\text{C}]1\text{b,c}$ bearing methoxy groups to tune
 98 the redox potential of the CDS. The preparation and *in vivo*
 99 evaluation of a 1,4-dihydroquinoline $[^{11}\text{C}]1\text{d}$ having a self-
 100 immolative linker between the CDS and MIBG will be also
 101 reported (Figure 1).

102 To perform the radiosynthesis and *in vivo* study of our
 103 systems, it was first necessary to synthesize the precursors for
 104 radiolabeling and references that will be used to identify
 105 compounds in radio-HPLC. We have previously described the
 106 synthesis of the targeting system **1a** starting from quinoline **4a**
 107 (Scheme 1).¹⁵ We decided to adopt the same approach to
 108 prepare **1b,c**. Thus, a coupling reaction from quinolines
 109 **4b,c**^{18,19} and MIBG using CDI led to the corresponding
 110 quinolines **5b,c** in moderate yields (36% and 30%,
 111 respectively). Alternatively, quinoline **5c** could be prepared

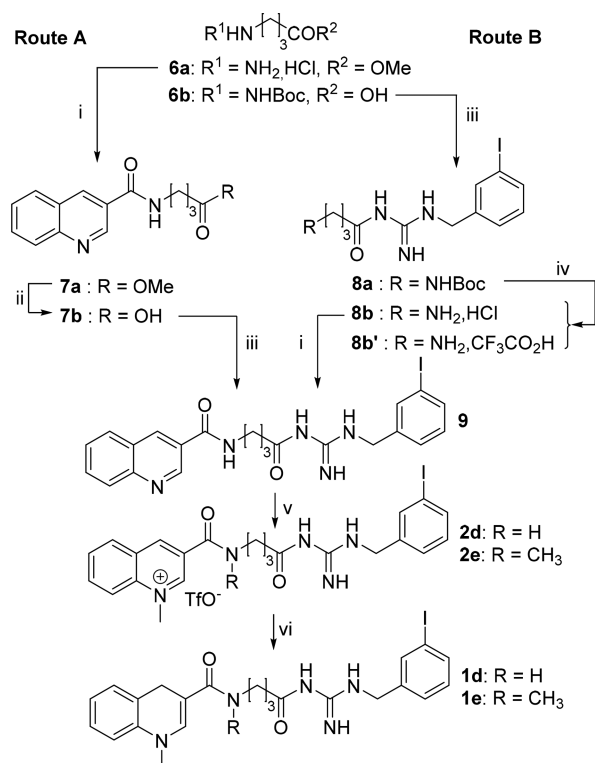
Scheme 1. Synthesis of the Redox CDS-MIBG **1a–c**^a



^aReagents and conditions: (i) CDI, DMF, 20 °C, 1 h then MIBG, 20 °C, 1 h for **5a*** (60%) and **5b** (36%) and **5c** (30%); (ii) NBI, NET_3 , DMF, 20 °C, 12 h (74%); (iii) MIBG, DMF, 140 °C, 7 h (76%); (iv) CH_3OTf , CH_2Cl_2 , 20 °C, 2 h for **2a*** (50%), 3 h for **2b** (60%) and **2c** (81%); (v) BNAH, CH_2Cl_2 , 20 °C, 12 h for **1a*** (95%), **1b** (32%), **1c** (70%). **1a***, **2a*** and **5a*** results are from ref 15.

by reacting MIBG with the activated enol ester²⁰ **4d** (76%),
 the latter having been obtained by reacting **4c** with NBI (74%).
 Then, quinolines **5b,c** were easily transformed into their
 corresponding quinolinium salts **2b,c** (60% and 81%,
 respectively) in the presence of methyl triflate. Finally, the
 desired CDS-MIBG **1b,c** were successfully obtained after
 regioselective reduction of quinolinium salts **2b,c** by means of
 BNAH (32% and 70%, respectively).

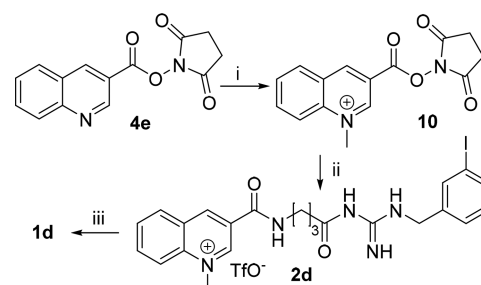
We next turned our attention to the synthesis of a CDS
 having a γ -aminobutyric acid (GABA) self-immolative linker
 group.^{21–23} We envisaged the synthesis of quinoline **9** from
 GABA derivative **6a** (Scheme 2, route A). So, neutralization of
 hydrochloride amine salt **6a** and subsequent coupling reaction
 with carboxylic acid **4a** using BOP reagent led to quinoline **7a**

Scheme 2. Initial Routes To Synthesize the Targeting System 1d^a

^aReagents and conditions: (i) NaOH then 4a, BOP, NEt₃, DMF, 20 °C, 12 h (79% for 7a, 25% for 9); (ii) LiOH, THF, MeOH, H₂O, 20 °C, 3 h (96%); (iii) BOP, MIBG, NEt₃, DMF, 20 °C, 12 h (25% for 8a, 4% for 9); (iv) CH₃COCl, MeOH, 20 °C, 1 h for 8b (95%) or TFA, CH₂Cl₂, -5 °C, 1 h for 8b' (98%); (v) CH₃OTf, CH₂Cl₂, 20 °C, 12 h (44% for 2d and 23% for 2e determined by ¹H NMR); (vi) BNAH, CH₂Cl₂, 20 °C, 12 h.

(79% yield). The methyl ester functional group was hydrolyzed by LiOH to give carboxylic acid 7b (96% yield). The latter was subsequently involved in a coupling reaction with MIBG using BOP to give 9 in a very low yield (4% yield). We also investigated other activation strategies of carboxylic acid 7b by means of CDI, ClCOOEt, (COCl), NBI, or NHS/DCC. Unfortunately, we failed to obtain 9 by using these reagents. Alternatively, *N*-protected GABA 6b and MIBG were reacted in the presence of BOP reagent to furnish the coupling product 8a in 25% yield (Scheme 2, route B). Then, *N*-Boc deprotection was carried out by using either acetyl chloride/MeOH or TFA to lead, respectively, to the desired ammonium salts 8b and 8b' (95% and 98% yields). One may note that 20 equiv of acetyl chloride/MeOH or TFA were required during the course of the *N*-Boc deprotection to prevent from the formation of the undesired γ -lactam ring resulting from the cyclization reaction of the self-immolative linker. Thereafter, ammonium 8b was neutralized back to pH 7 with sodium hydroxide before being converted into the desired amide 9 in 25% yield by means of a coupling reaction between 4a and BOP reagent. The quaternization reaction of 9 with methyl triflate afforded a mixture of 2d,e (44% and 23%, respectively, estimated by ¹H NMR). We then proceeded to a classical reduction of the mixture of quinolinium salts 2d,e with BNAH. However, LC/MS analysis of the crude reaction medium revealed the presence of both 1,4-dihydroquinolines 1d,e and

quinolinium salts 2d,e, which turned out to be extremely difficult to separate. Given this result, we decided to explore another route to obtain exclusively 1,4-dihydroquinoline 1d. To overcome the alkylation reaction leading to undesirable 2e, quinoline 4e was first quaternized with methyl triflate to give the key intermediate 10 in 96% yield (Scheme 3). The resulting NHS-activated quinolinium 10²⁴ was

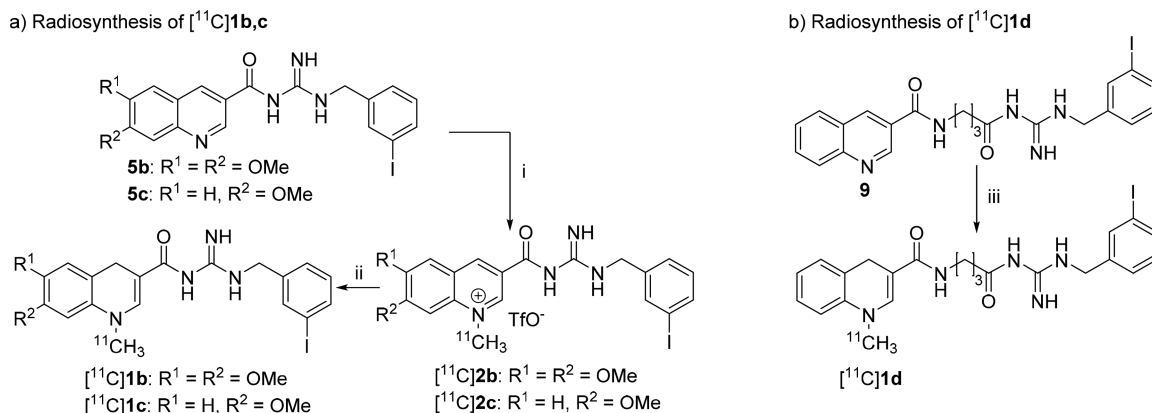
Scheme 3. Alternative Route to the Redox CDS-MIBG 1d^a

^aReagents and conditions: (i) CH₃OTf, CH₂Cl₂, 20 °C, 4 h (96%); (ii) polymer-bound DBU, 8b', THF, 20 °C, 12 h (58%); (iii) BNAH, CH₂Cl₂, 20 °C, 4 h (77% determined by ¹H NMR).

smoothly reacted with linker-MIBG derivative 8b' to yield compound 2d (58%). Finally, a classical reduction reaction with BNAH led to the desired MIBG-targeting system 1d (77% determined by ¹H NMR).

Radiosyntheses of [¹¹C]1b,c were carried out as depicted in Scheme 4 according to a two-step synthetic procedure.^{15,16,25} The structures of the ¹¹C-labeled products were confirmed by comparing their retention time with the corresponding nonradioactive standard compounds using reverse-phase HPLC. Thus, the quaternization reaction of quinolines 5b,c with [¹¹C]methyl triflate afforded quinolinium salts [¹¹C]2b,c. Reduction of [¹¹C]2b,c was conducted with BNAH for 5 min at 100 °C to provide the corresponding 1,4-dihydroquinolines [¹¹C]1b,c (respectively, 68% and 61% relative percentages determined by radio-HPLC). The same procedure was applied to the radiosynthesis of [¹¹C]1d. However, radio-HPLC analyses demonstrated that [¹¹C]2d was not stable enough under these high dilution reaction conditions. To circumvent the poor stability of [¹¹C]2d, we decided to add the reducing agent BNAH and the alkylating agent [¹¹C]CH₃OTf simultaneously. Then, the reaction mixture was left to react 5 min at 20 °C. To prevent [¹¹C]1d from oxidation during the purification step, basic HPLC conditions were required. So, by adding triethylamine in HPLC eluent, 1,4-dihydroquinoline [¹¹C]1d was obtained with a radiochemical purity of 50% (based on HPLC analysis of the crude product). A TRACERlab FX-MeI and FX-M radiosynthesis module was used to achieve a fully automated radiosynthesis of [¹¹C]1b-d using a two-step reaction as shown in Scheme 4. The total synthesis time of the fully automated process was approximately 50 min. Activity levels in the final product ranged from 592 to 814 MBq for [¹¹C]1b; 259–444 MBq for [¹¹C]1c; and 148–518 MBq for [¹¹C]1d. The radiochemical purities of [¹¹C]1b-d were >95%.

Then, biological studies were conducted in rats to determine, *in vivo*, the cerebral penetration through the BBB of the different MIBG-targeting systems [¹¹C]1b-d by measuring the radioactivity of the cerebral samples obtained after sacrifice of the animals (Figure 2). Last but not least, we

Scheme 4. Radiosyntheses of $[^{11}\text{C}]1\text{b-d}^a$ 

^aReagents and conditions: for $[^{11}\text{C}]1\text{b,c}$ from **5b,c**: (i) $[^{11}\text{C}]\text{CH}_3\text{OTf}$, CH_3CN , $20\text{ }^\circ\text{C}$, 5 min; (ii) BNAH, CH_3CN , $100\text{ }^\circ\text{C}$, 5 min; for $[^{11}\text{C}]1\text{d}$ from **9**: (iii) $[^{11}\text{C}]\text{CH}_3\text{OTf}$, CH_3CN , $20\text{ }^\circ\text{C}$ and BNAH, then 10 min, $20\text{ }^\circ\text{C}$.

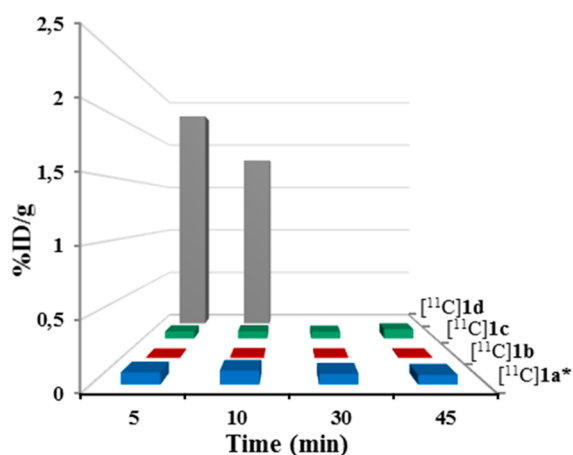


Figure 2. *Ex vivo* biodistribution of the radioactivity in rat brain at different time intervals following tail vein injection of $[^{11}\text{C}]1\text{a-d}$ (5, 10, 30, and 45 min for $[^{11}\text{C}]1\text{a-c}$; 5 and 10 min for $[^{11}\text{C}]1\text{d}$). Results are expressed in percent of injected dose per gram (%ID/g, mean, $n = 2$ for each point). $[^{11}\text{C}]1\text{a}^*$ results are from ref 15.

quinolinium salts $[^{11}\text{C}]2\text{b-d}$, which subsequently led to the 200 cleavage of MIBG from the carrier through hydrolysis. The 201 results will be compared to those already obtained from $[^{11}\text{C}]$ 202 **1a**¹⁵ in order to select the most promising CDS to target 203 MIBG to the CNS. 204

Then, the monitoring of both oxidation and MIBG cleavage 205 steps in the CNS were investigated from brain samples, which 206 were analyzed by radio-HPLC after radiotracer injection. Both 207 CDS-MIBG $[^{11}\text{C}]1\text{b}$ and $[^{11}\text{C}]1\text{c}$ proved to be rather stable 208 since 87% and 90% of 1,4-dihydroquinolines $[^{11}\text{C}]1\text{b,c}$, 209 respectively, were detected at 10 min after injection, together 210 with 12% and 5% of quinolinium salts $[^{11}\text{C}]2\text{b,c}$, respectively, 211 but with no traces of carboxylic acids $[^{11}\text{C}]3\text{b,c}$ (Figure 3b,c). 212 ¹⁵ Regarding CDS-MIBG $[^{11}\text{C}]1\text{a}$ previously investigated,¹⁵ the 213 percentage of carboxylic acid $[^{11}\text{C}]3\text{a}$ reached 11% at 10 min 214 after injection, highlighting a faster cleavage of MIBG from the 215 quinolinium salt **2a** (Figure 3a). We can therefore draw the 216 conclusion that the presence of methoxy groups on the carrier 217 do not increase the oxidation rates of $[^{11}\text{C}]1\text{b,c}$ in the brain 218 compared to $[^{11}\text{C}]1\text{a}$ and even seems to delay the cleavage of 219 MIBG from the resulting quinolinium salts $[^{11}\text{C}]2\text{b,c}$. 220

At this stage, it seems that in terms of brain uptake, 221 oxidation, and hydrolysis rates, CDS-MIBG $[^{11}\text{C}]1\text{a}$ remains 222 the best candidate among the three CDS-MIBG $[^{11}\text{C}]1\text{a-c}$. In 223

198 were also interested (both in brain and plasma) in the 199 oxidation rates of $[^{11}\text{C}]1\text{b-d}$ into the corresponding

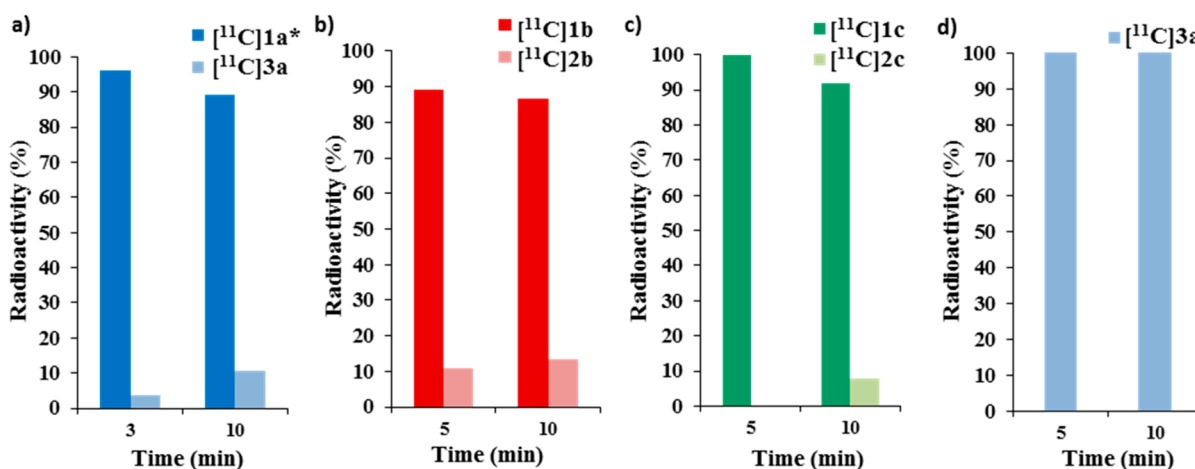
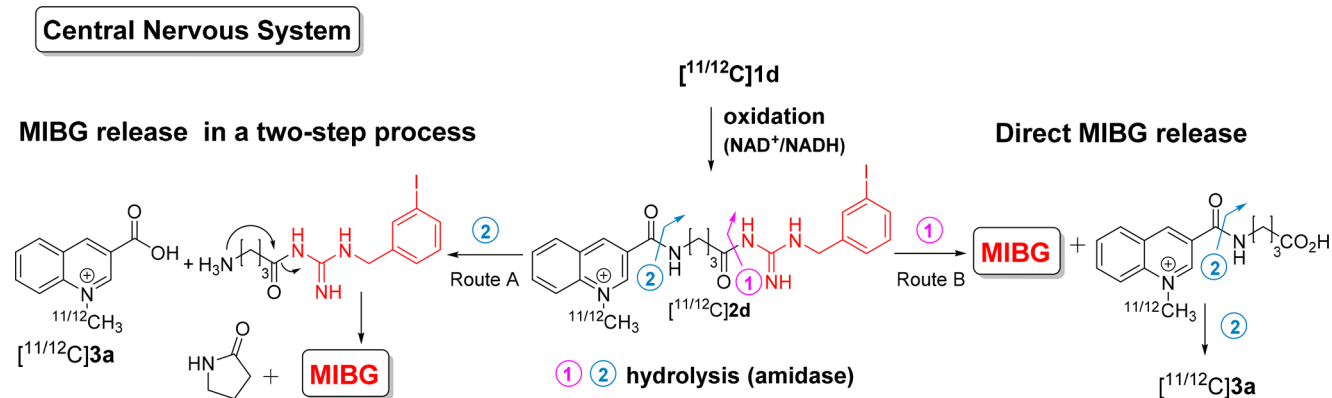


Figure 3. Percentage of the expected $[^{11}\text{C}]$ radioactive species in brain after injection into rat of (a) $[^{11}\text{C}]1\text{a}$, (b) $[^{11}\text{C}]1\text{b}$, (c) $[^{11}\text{C}]1\text{c}$, and (d) $[^{11}\text{C}]1\text{d}$ (mean, $n = 2$ for each time point). $[^{11}\text{C}]1\text{a}^*$ results are from ref 15.

Scheme 5. Schematic Representation for MIBG Release from Carrier-linker-MIBG 1d



224 contrast, HPLC analyses of both brain and plasma samples at 5
 225 min after injection of 1,4-dihydroquinoline [^{11}C]1d revealed
 226 the presence of only one polar radioactive compound
 227 corresponding to the carboxylic acid [^{11}C]3a (Figure 3d).
 228 These data indicate a fast *in vivo* oxidation of [^{11}C]1d followed
 229 by hydrolysis of the resulting quinolinium salt [^{11}C]2d leading
 230 to the release of carboxylic acid [^{11}C]3a along with the linker-
 231 MIBG intermediate, which would undergo cyclization to
 232 produce desired MIBG along with γ -lactam as byproduct. This
 233 scenario depicted in Scheme 5 (route A) is backed up by the
 234 fact that during the preparation of 8b,b', a fast cyclization
 235 process of the corresponding free amine was observed leading
 236 to MIBG and γ -lactam products. At this stage, a second
 237 scenario cannot be ruled out in which hydrolysis would occur
 238 at the carbonyl group attached to MIBG as shown in Scheme 5
 239 (route B) to release MIBG in a single step. In light of our
 240 results, it might be concluded that the presence of a linker
 241 between the 1,4-dihydroquinoline moiety and MIBG increases
 242 notably not only the BBB passage and oxidation rate of [^{11}C]
 243 1d but also the release of MIBG from the carrier in the brain.
 244 In this study, we successfully synthesized and labeled with
 245 carbon-11 various [^{11}C]CDS-MIBG ([^{11}C]1b–d). We also
 246 examined *in vivo* their potential to deliver MIBG into the
 247 central nervous system. A preclinical evaluation showed high
 248 BBB permeability of the carrier-linker-MIBG [^{11}C]1d as
 249 demonstrated by the high percentage of radioactivity measured
 250 in the brain, whereas the two other CDS-MIBG [^{11}C]1b,c
 251 exhibited poor BBB passage. Once in the brain, fast oxidation
 252 of the 1,4-dihydroquinoline [^{11}C]1d and prompt cleavage of
 253 MIBG from the resulting quinolinium salt [^{11}C]2d take place
 254 as evidenced by the only presence of carboxylic acid [^{11}C]3a in
 255 brain samples after 5 min. In light of these promising *in vivo*
 256 profiles observed with [^{11}C]1d, this work paves the way to the
 257 use of the CDS-radiolabeled-MIBG as an appealing imaging
 258 tool for the study of cerebral adrenergic nerve endings within
 259 the brain.²⁶²⁷²⁸²⁹

260 ■ ASSOCIATED CONTENT

261 ● Supporting Information

262 The Supporting Information is available free of charge on the
 263 ACS Publications website at DOI: 10.1021/acsmchem-
 264 lett.8b00642.

265 Experimental procedures and characterization of all
 266 compounds, radiosyntheses and procedures for *in vivo*
 267 experiments (PDF)

■ AUTHOR INFORMATION

Corresponding Authors

*E-mail: gourand@cyceron.fr.

*E-mail: vincent.levacher@insa-rouen.fr.

ORCID

Fabienne Gourand: 0000-0002-3585-6437

Vincent Levacher: 0000-0002-6429-1965

Author Contributions

The manuscript was written through contributions of all authors. All authors have given approval to the final version of the manuscript;

Notes

The authors declare no competing financial interest.

■ ACKNOWLEDGMENTS

This study was supported by a grant from CEA (Commissariat à l'Énergie Atomique et aux Énergies Alternatives), Labex IRON (ANR-11-LABX-0018-01), INSA-Rouen, Rouen University, CNRS, Labex SynOrg (ANR-11-LABX-0029), and Région Normandie. D.P. was supported by a grant "CIFRE" from Région Basse-Normandie and Cyclopharma laboratories. A.H. was supported by a grant from Région Haute-Normandie (Grant: CRUNCH 6-13).

■ ABBREVIATIONS

MIBG, *meta*-iodobenzylguanidine; NET, norepinephrine transporter; BBB, blood–brain barrier; CDS, chemical delivery system; SPECT, single photon emission computed tomography; PET, positron emission tomography; CNS, central nervous system; ADHD, attention deficit hyperactivity disorder

■ REFERENCES

- (1) Goldstein, D. S.; Eisenhofer, G.; Flynn, J. A.; Wand, G.; Pacak, K. Diagnosis and Localization of Pheochromocytoma. *Hypertension* **2004**, *43*, 907–910.
- (2) Cryer, P. E. Pheochromocytoma. *West. J. Med.* **1992**, *156*, 399–407.
- (3) Brisse, H.; Edeline, V.; Michon, J.; Couanet, D.; Zucker, J.; Neuenschwander, S. Current strategy for the imaging of neuroblastoma. *J. Radiol.* **2001**, *82*, 447–54.
- (4) Zhang, H.; Huang, R.; Pillarsetty, N.; Thorek, D. L.; Vaidyanathan, G.; Serganova, I.; Blasberg, R. G.; Lewis, J. S. Synthesis and evaluation of 18F-labeled benzylguanidine analogs for targeting the human norepinephrine transporter. *Eur. J. Nucl. Med. Mol. Imaging* **2014**, *41*, 322–332.

- (5) Zhang, H.; Huang, R.; Cheung, N.-K. V.; Guo, H.; Zanzonico, P. B.; Thaler, H. T.; Lewis, J. S.; Blasberg, R. G. Imaging the Norepinephrine Transporter in Neuroblastoma: A Comparison of [18F]-MFBG and 123I-MIBG. *Clin. Cancer Res.* **2014**, *20*, 2182–2191.
- (6) Hu, B.; Vavere, A. L.; Neumann, K. D.; Shulkin, B. L.; DiMagno, S. G.; Snyder, S. E. A Practical, Automated Synthesis of meta-[18F]Fluorobenzylguanidine for Clinical Use. *ACS Chem. Neurosci.* **2015**, *6*, 1870–1879.
- (7) Pandit-Taskar, N.; Zanzonico, P.; Staton, K. D.; Carrasquillo, J. A.; Reidy-Lagunes, D.; Lyashchenko, S.; Burnazi, E.; Zhang, H.; Lewis, J. S.; Blasberg, R.; Larson, S. M.; Weber, W. A.; Modak, S. Biodistribution and Dosimetry of 18F-Meta-Fluorobenzylguanidine: A First-in-Human PET/CT Imaging Study of Patients with Neuroendocrine Malignancies. *J. Nucl. Med.* **2018**, *59*, 147–153.
- (8) Baulieu, J. L.; Huguet, F.; Chalon, S.; Gerard, P.; Frangin, Y.; Besnard, J. C.; Pourcelot, L.; Guilloteaue, D. [¹²⁵I]MIBG uptake and release in different regions of the rat brain. *Nucl. Med. Biol.* **1990**, *17*, 511–514.
- (9) Prokai, L.; Prokai-Tatrai, K.; Bodor, N. Targeting drugs to the brain by redox chemical delivery systems. *Med. Res. Rev.* **2000**, *20*, 367–416.
- (10) Bodor, N.; Buchwald, P. Barriers to remember: brain-targeting chemical delivery systems and Alzheimer's disease. *Drug Discovery Today* **2002**, *7*, 766–774.
- (11) Bodor, N.; Venkatraghavan, V.; Winwood, D.; Estes, K.; Brewster, M. E. Improved delivery through biological membranes. XLI. Brain-enhanced delivery of chlorambucil. *Int. J. Pharm.* **1989**, *53*, 195–208.
- (12) Wu, W. M.; Pop, E.; Shek, E.; Bodor, N. Brain-specific chemical delivery systems for beta-lactam antibiotics. In vitro and in vivo studies of some dihydropyridine and dihydroisoquinoline derivatives of benzylpenicillin in rats. *J. Med. Chem.* **1989**, *32*, 1782–1788.
- (13) Pop, E.; Bodor, N. Chemical systems for delivery of antiepileptic drugs to the central nervous system. *Epilepsy Res.* **1992**, *13*, 1–16.
- (14) Bodor, N.; Buchwald, P. *Soft Drugs in Retrometabolic Drug Design and Targeting*; John Wiley & Sons, Inc.: Hoboken, NJ, 2012.
- (15) Gourand, F.; Mercey, G.; Ibazizène, M.; Tirel, O.; Henry, J.; Levacher, V.; Perrio, C.; Barré, L. Chemical delivery system of Metaiodobenzylguanidine (MIBG) to the central nervous system. *J. Med. Chem.* **2010**, *53*, 1281–1287.
- (16) Gourand, F.; Țințaș, M.-L.; Henry, A.; Ibazizène, M.; Dhilly, M.; Fillesoye, F.; Papamicaël, C.; Levacher, V.; Barré, L. Delivering FLT to the Central Nervous System by Means of a Promising Targeting System: Synthesis, [¹¹C]Radiosynthesis and *in Vivo* Evaluation. *ACS Chem. Neurosci.* **2017**, *8*, 2457–2467.
- (17) Tedjamulia, M. L.; Srivastava, P. C.; Knapp, F. F., Jr. Evaluation of the brain-specific delivery of radioiodinated (iodophenyl) alkyl-substituted amines coupled to a dihydropyridine carrier. *J. Med. Chem.* **1985**, *28*, 1574–1580.
- (18) Benoit, R.; Dupas, G.; Bourguignon, J.; Quéguiner, G. Facile synthesis of annelated NADH model precursors. *Synthesis* **1987**, *12*, 1124–1126.
- (19) Charpentier, P.; Lobregat, V.; Levacher, V.; Dupas, G.; Quéguiner, G.; Bourguignon, J. An efficient synthesis of 3-cyanoquinoline derivatives. *Tetrahedron Lett.* **1998**, *39*, 4013–4016.
- (20) Woodman, D. J.; Davidson, A. I. N-Acylation during the addition of carboxylic acids to N-tert-butylacetylketenimines and the use of the reagent N-tert-butyl-5-methylisoxazolium perchlorate for peptide synthesis. *J. Org. Chem.* **1973**, *38*, 4288–4295.
- (21) Zhang, X.-B.; Waibel, M.; Hasserodt, J. An autoimmolative spacer allows first-time incorporation of a unique solid-state fluorophore into a detection probe for acyl hydrolases. *Chem. - Eur. J.* **2010**, *16*, 792–795.
- (22) DeWit, M. A.; Gillies, E. R. Design, synthesis, and cyclization of 4-aminobutyric acid derivatives: potential candidates as self-immolative spacers. *Org. Biomol. Chem.* **2011**, *9*, 1846–1854.
- (23) Alouane, A.; Labruère, R.; Le Saux, T.; Schmidt, F.; Jullien, L. Self-immolative spacers: kinetic aspects, structure-property relationships, and applications. *Angew. Chem., Int. Ed.* **2015**, *54*, 7492–7509.
- (24) Barré, A.; Țințaș, M.-L.; Levacher, V.; Papamicaël, C.; Gembus, V. An overview of the synthesis of highly versatile N-hydroxysuccinimide esters. *Synthesis* **2017**, *49*, 472–483.
- (25) Bohn, P.; Gourand, F.; Papamicaël, C.; Ibazizène, M.; Dhilly, M.; Gembus, V.; Alix, F.; Tintas, M.-L.; Marsais, F.; Barré, L.; Levacher, V. Dihydroquinoline carbamate derivatives as bio-oxidizable >> prodrugs for brain delivery of acetylcholinesterase inhibitors: [¹¹C] radiosynthesis and biological evaluation. *ACS Chem. Neurosci.* **2015**, *6*, 737–744.
- (26) Jewett, D. M. A simple synthesis of [¹¹C]methyl triflate. *Int. J. Rad. Appl. Instrum. A* **1992**, *43*, 1383–1385.
- (27) Mauzerall, D.; Westheimer, F. H. 1-Benzylidihydronicotinamide - A model for reduced DPN. *J. Am. Chem. Soc.* **1955**, *77*, 2261–2264.
- (28) Wieland, D. M.; Wu, J.-L.; Brown, L. E.; Mangner, T. J.; Swanson, D. P.; Beierwaltes, W. H. Radiolabeled adrenergic neuron-blocking agents: adrenomedullary imaging with [¹³¹I]-Iodobenzylguanidine. *J. Nucl. Med.* **1980**, *21*, 349–353.
- (29) Wieland, D. M.; Mangner, T. J.; Inbasekaran, M. N.; Brown, L. E.; Wu, J.-L. Adrenal medulla imaging agents: a structure-distribution relationship study of radiolabeled aralkylguanidines. *J. Med. Chem.* **1984**, *27*, 149–155.